OPTOELECTRONICS AND ADVANCED MATERIALS – RAPID COMMUNICATIONS Vol. 1, No. 8, August 2007, p. 379 - 384

A study of the optical response speed of silicon Bulk - Barrier photodiodes based on simulation results

P. PAPADOPOULOU[a], N. GEORGOULAS[b], L. MAGAFAS[c]
[a]*Department of Science, Technological Educational Institute of Kavala, St. Loukas 65404 Kavala, Greece. E-mail:*
[b]*Laboratory of Electrical and Electronic Materials Technology, Department of Electrical and Computer Engineering, Democritus University of Thrace, 67100, Xanthi, Greece*
[c]*Department of Electrical Engineering, Technological Educational Institute of Kavala, St. Loukas 65404 Kavala, Greece.*

In this paper, an extensive study of the transient optical response speed of silicon Bulk–Barrier Diodes (BBDs) is presented. This study is based on the simulation results obtained with a 2-D device simulator (S-PISCES and LUMINOUS). The influence of significant quantities, as the applied voltage, the incident light power and the light wavelength, on the optical response speed of silicon Bulk–Barrier Diodes was investigated. As a result of this study we propose a model that calculates the cut–off frequency (optical response speed) of silicon BBDs when a modulated light is applied. Simulation results verify the validity of the proposed model and show that it is possible to achieve high speed optical response by choosing appropriate operational parameters.

(Received April 9, 2007; accepted June 26, 2007)

Keyword: Bulk-Barrier Diodes, Silicon photodiodes, optical response speed, Device Simulation

1. Introduction

High-speed and high-sensitivity photodetectors are required for high bit-rate optical communication systems. The most commonly used photodetectors in these systems are avalanche photodiodes, p-i-n photodiodes and phototransistors. Because avalanche photodiode has internal gain, it offers the most sensitive receivers at lower frequencies. A p-i-n photodetector is structurally very simple and the speed of this device depends on the intrinsic layer. For high speed operation this layer should be completely depleted [1]. Even though silicon phototransistors show high linearity and sensitivity [2], they present low optical gain and slow response speed, due to the minority carrier storage in the neutral base region.

Several types of photodetectors with high sensitivity and quantum efficiency have been developed for optical communications [3-5]. Among these are devices like the a -SiC:H bulk barrier color detector [7], the npn heteroctructure optoelectronic switch [8], the majority – carrier camel diode or the bulk barrier diode [3-15].

Several published models describe the electrical and optoelectronic properties of such structures [3-7, 9, 12]. However, there are only few studies on the optical response speed and the transient behavior of these structures under pulse illumination [7].

In this paper, we present an extensive study of the optical response speed of silicon Bulk – Barrier Diodes (BBDs) using simulation results. Based on the model presented in previous works [6, 12], we have developed an analytical model, which accurately describes the silicon BBD's cut–off, f_c, frequency (optical response speed) when a modulated light is applied, as a function of the applied bias voltage, the incident light power level, the wavelength and the technological parameters. Advanced simulation packages (S- PISCES and LUMINOUS) were used to investigate the optical response and to verify the validity of the proposed analytical model.

2. Theory

Camel diodes or bulk barrier diodes operate as majority-carrier devices, where the current transport is controlled by the potential barrier height located in the interior of the semiconductor. It is possible to control this height by free carriers trapped in the potential minimum (potential well). Their presence in the middle layer lowers the potential barrier and allows more majority carriers to be injected here from the p^+ layer, from where they are swept into the bulk material (p layer). These carriers can be generated optically within the space charge region and the adjacent diffusion regions. The excess carriers will be stored in the potential minimum until they vanish by recombination and back injection into the anode. In this way the optically generated carriers control the current flow in the diode, by reducing the potential barrier, and lead to a high internal photocurrent gain. In general, the gain increases with increasing storage times.

Fig. 1 (a) and (b) shows schematically the structure and the corresponding energy band diagram of a BBD with reverse bias, under dark (——) and illumination (– – –) conditions. In these figures d is the BBD's middle layer thickness, N_E, N_B, and N_C are the doping levels of the emitter (p^+ layer), base (n layer) and collector (substrate) regions. For reverse bias (i.e. with + on the p^+ layer and -

on the p-substrate) the depletion layer width in the substrate expands, the potential barrier height on the right side, Φ_{BR}, increases linearly with the applied voltage, whereas the potential barrier height on the left side, Φ_{BL} [6,12], decreases. In this case the current transport is determined by the injection of holes from the p^+ layer, which have to overcome the lowest barrier.

The dark current density of BB diode in the reverse bias, J_{DR}, is given by [6, 12]:

$$J_{DR} = J_{SR} \cdot \exp\left(-\frac{q \cdot \Phi_{BL}}{kT}\right) \quad , \quad \text{for } |V_R| > \frac{3 \cdot kT}{q} \qquad (1)$$

where J_{SR} is the saturation current density, q is the electron charge, k is the Bultzmann constant, T is the absolute temperature, V_R is the reverse applied voltage.

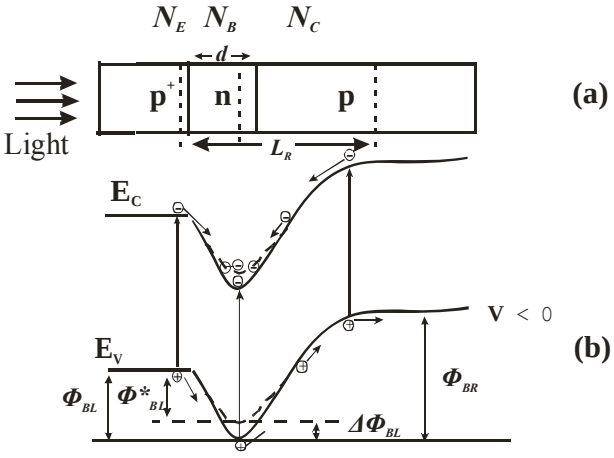

Fig. 1. (a) Schematic diagram of a BBD structure and (b) energy band diagram of a BBD structure with reverse bias, under dark (———) and illumination conditions (– – –).

Consider photons with energy greater than the silicon energy band gap, which fall on the p^+ layer side. These photons will generate electron-hole pairs, mainly in the middle layer and in the substrate region (the p^+ layer has a thickness smaller than 100nm). Photogenerated holes will drift down to the substrate (see Fig.1) and, finally, they will be collected by the back electrode (primary photocurrent). On the other hand, the photogenerated electrons drift down to the energy conduction band minimum, where they are trapped. The excess electron density in the middle layer reduces the donor charges, and thus induces a barrier height lowering, $\Delta\Phi_{BL}$. This barrier height lowering leads to a significant increase of the diode current density, J_{DR}, according to eq.(1). This current density is called secondary photocurrent density, J_{PH} , and it is given by [6, 12]:

$$J_{PH} = J_{DR} \cdot \left[\exp\left(\frac{q \cdot \Delta\Phi_{BL}}{kT}\right) - 1\right] \qquad (2)$$

In the steady state, the total electron flux moving towards the energy conduction band minimum should be equal to that leaving this energy minimum. Under illumination conditions (quantities are symbolized with an asterisk *), the continuity equation leads to the following expression [6, 12]:

$$\frac{\eta_0 \cdot P_i}{h\nu} + \frac{J_{nd}}{q} = \frac{S_n^*}{\tau_{eff}^*} \qquad (3)$$

with

$$S_n^* = \sqrt{2\pi} \cdot L_{DB} \cdot n_{B0}^* \qquad (4)$$

The first term on the left hand side of eq.(3) is the primary photocurrent density ($J_L=\eta_0 P_i / h\nu$), J_{nd} is the electron current density under dark conditions, P_i the optical power density, η_0 the total internal quantum efficiency, $h\nu$ the photon energy, τ^*_{eff} the electron effective lifetime in their accumulation region, L_{DB} is the Debye length, S^*_n is the surface electron density calculated over a Debye length, and n^*_{B0} the electron density at the potential maximum given by [6,12].

$$n_{B0}^* = n_{B0} \cdot \exp\left(\frac{q \cdot \Delta\Phi_{BL}}{kT}\right) \qquad (5)$$

The lifetime of photogenerated electrons depends on their loss mechanisms. The electrons can leave the conduction band well by several mechanisms. First, electrons can recombine with holes, which are injected from the p^+ layer into the middle layer, or they can escape from the energy well by diffusion back to the p^+ layer. For τ_{eff}^* we can write:

$$\frac{1}{\tau_{eff}^*} = \frac{1}{\tau_{rec}^*} + \frac{1}{\tau_{diff}^*} \qquad (6)$$

where τ^*_{rec} and τ^*_{diff} are the lifetimes associated with the recombination and diffusion processes of the accumulated electrons, respectively.

The recombination current density of a BBD under dark conditions is given by [6, 12]:

$$J_{rec} = \frac{1}{2\tau} \cdot q \cdot \sqrt{2\pi} \cdot L_{DB} \cdot \sqrt{p_E \cdot n_{B0}} \cdot \exp\left(-\frac{q \cdot \Phi_{BL}}{2 \cdot kT}\right) \qquad (7)$$

where p_E, is the hole concentration in the p^+ region, τ is the lifetime of the trapped carriers [6,12].

The diffusion of accumulated electrons, back to the p^+ layer, can be expressed by the dark diffusion current density [6, 12]:

$$J_{diff} = \frac{q \cdot D_{nE} \cdot n_{B0}}{d + (D_{nE}/D_{nB}) \cdot \sqrt{\pi/2} \cdot L_{DB}} \cdot \exp\left(-\frac{q \cdot \Phi_{BL}}{kT}\right) \qquad (8)$$

where D_{nE} and D_{nB} are the diffusion constants for electrons in the p^+ and n regions, respectively.

Substituting eq.(5) into (4), using equations (6), (7), (8), as well as the expressions $J^*_{rec} = (qS^*_n/\tau^*_{rec})$ and $J^*_{diff} = (qS^*_n/\tau^*_{diff})$, we can calculate the electron effective

lifetime, τ^*_{eff}, and further more the cut-off frequency, f_c, ($f_c = 1/(2\pi\,\tau^*_{eff})$), from the following form:

$$f_c = \frac{1}{2\pi\cdot\tau^*_{eff}} = \frac{1}{2\pi}\cdot\left(\frac{1}{\tau^*_{rec}} + \frac{1}{\tau^*_{diff}}\right) = \frac{J_{rec}}{2\pi\cdot q\cdot S_n} + \frac{J_{diff}}{2\pi\cdot q\cdot S_n}\cdot\exp\left(\frac{q\cdot\Delta\Phi_{BL}}{kT}\right) \quad (9)$$

Here $\Delta\Phi_{BL}$ is given by the relation [12]:

$$\Delta\Phi = \frac{kT}{q}\cdot\ln\left(1 + \frac{P_i}{P_{i0}}\right)^m \quad (10)$$

with

$$P_{i0} = \frac{J_{nd}\cdot hv}{\eta_0\cdot q} \quad \text{and} \quad \frac{1}{2} \le m \le 1 \quad (11)$$

For the case of m=1 the dominant transport mechanism is recombination whereas for m=1/2 it is drift diffusion [6, 12].

Substitution of eq. (10) in eq. (9) gives:

$$f_c = \frac{1}{2\pi\cdot\tau^*_{eff}} = \frac{1}{2\pi}\cdot\left(\frac{1}{\tau^*_{rec}} + \frac{1}{\tau^*_{diff}}\right) = \frac{J_{rec}}{2\pi\cdot q\cdot S_n} + \frac{J_{diff}}{2\pi\cdot q\cdot S_n}\cdot\left(1+\frac{P_i}{P_{i0}}\right)^m \quad (12)$$

Equation (12) indicates that the cut-off frequency, f_c, of a Bulk-Barrier photodiode under pulse illumination is a function of the optical power density P_i. For high optical power levels ($P_i >> P_{i0}$), eq. (12) shows that the cut–off frequency f_c, increases as the optical power density falling on the BBD increases. On the othetr side, for low optical power levels ($P_i << P_{i0}$,) and for exponent term (m)<1 the bracket in eq. (12) tends to unity, since $P_i / P_{i0} << 1$ [16], showing that the cut–off frequency f_c, does not depend on the optical power density P_i falling on the BBD structure.

The external quantum efficiency, η_{ext}, can be defined by the relation in [6, 12]:

$$\eta_{ext} = \frac{I_{PH}}{P_i}\cdot\frac{hv}{q} \quad (13)$$

3. Simulation results

In this work we investigate for the first time the validity of the proposed model and the influence of the various operational and technological parameters on the cut–off frequency f_c (optical response speed) of silicon Bulk – Barrier Diodes (BBDs) using advanced simulation programs such as S-PISCES and LUMINOUS (SILVACO) which work under ATLAS framework.

ATLAS is a physically-based device simulator. Physically-based device simulators predict the electrical characteristics that are associated with specified physical structures and bias conditions. This is achieved by approximating the operation of a device onto a two or three dimensional grid, consisting of a number of grid points called nodes. By applying a set of differential equations, derived from Maxwell's laws, onto this grid you can simulate the transport of carriers through a structure.

The S-PISCES that simulates the electrical characteristics of silicon semiconductor devices in steady-state, transient and AC conditions, the device structures may be specified by the user. LUMINOUS used with S-PISCES calculates optical intensity profiles within the semiconductor device and converts these profiles into photogeneration rates, allowing thus to simulate device electronic responses to optical signals. For the simulation, the drift-diffusion model was used, because the geometrical characteristics of the structures were much larger than the mean free path of carriers. In addition, for more accurate predictions of device performance, several physical models, such as concentration and field dependent mobility, Shockley-Read-Hall and Auger carrier recombination and band gap narrowing were employed.

It must be referred that in the present work the simulation results presented below do not use theoretical results from above.

Fig. 2 shows simulation results of the influence of the light modulation frequency f_M, on the external quantum efficiency η_{ext}, obtained from the S-PISCES and LUMINOUS data, for a BBD structure with d=100 nm, $N_E = 10^{19}$ cm^{-3}, $N_B = 10^{17}$ cm^{-3}, and $N_C = 10^{15}$cm^{-3}, with applied voltage V_R = – 6V, for optical power density $P_i = 5\cdot10^{-5}$ W/cm^2 and for a given light wavelength λ=0.65μm. It should be referred that the light modulation frequency f_M is a parameter related to the lifetime of the accumulated electrons [6, 12] and shows the response speed. In this figure, dots present simulation results of the quantum efficiency η_{ext}, and the dashed lines present the extrapolation of the two different mechanisms at low and high frequencies respectively. The first plateau, where the quantum efficiency takes high values ($\eta_{ext} >> 1$), which appears at low modulation frequencies, indicates the first mechanism, which is the photocurrent amplification mechanism (secondary photocurrent). As the light modulation frequency f_M, takes values lower than the cut-off frequency f_c, which is the frequency imposed by the electron effective lifetime τ^*_{eff}, in their accumulation region ($f_M < f_c = 1/(2\pi\,\tau^*_{eff})$) the quantum efficiency η_{ext} remains constant. The cut-off frequency f_c, is usually defined as the frequency where the investigated magnitude (e.g. quantum efficiency η_{ext}) becomes 3dB lower than its initial value [1, 17], and in the case of the BBD described by eq. (12). When the light modulation frequency f_M, becomes greater than the cut-off frequency f_c, then the modulation of the barrier height, $\Delta\Phi_{BL}$ can not follows the light modulation, and consequently leads to a decrease of the quantum efficiency according to eqs.(2), (13). The reduction of the external quantum efficiency continues, with a constant slope as the light modulation frequency f_M increases. For high modulation frequencies (f_M > 1MHz) the gain mechanism vanishes and the efficiency η_{ext} reaches the second plateau. This second plateau indicates the second mechanism related to the primary photocurrent ($\eta_{ext} \le 1$). In a p$^+$-n-p structure the primary photocurrent mechanism, is the photogenerated holes current which

drift down to the substrate and, finally, they collected by the back electrode, while the photogenerated electrons accumulate in the energy band well. The cut–off frequency of the primary photocurrent mechanism is determined by the discharge time of the depletion capacitance.

Fig. 3 shows simulation results of the quantum efficiency η_{ext}, obtained from the S-PISCES and LUMINOUS data, as a function of the light modulation frequency f_M, for different values of the optical power density P_i falling on a BBD, the other conditions being the same as for Fig. (2). It is obvious from this figure that the two different mechanisms can be observed for all curves. In the case of the photocurrent gain mechanism, the external quantum efficiency, for low modulation frequencies, remains constant and it takes high values (20 – 400), depending on optical incident power density P_i. It is obvious from this figure that the cut-off frequency f_c, depends on the incident optical power density P_i.

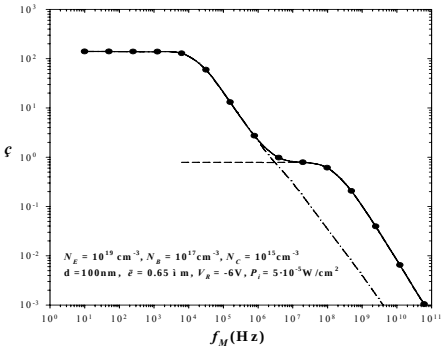

Fig. 2. S-PISCES-LUMINOUS simulation results of the external quantum efficiency, η_{ext}, as a function of the light modulation frequency, f_M (dots), and the extrapolation (dashed lines) of the two different mechanisms.

Based on simulation results of the quantum efficiency η_{ext}, as a function of the light modulation frequency for different values of the optical power density and wavelengths, is observed the cut-off frequency, f_c, as a function of the incident optical power density P_i and the results are presented in fig. (4). As this figure shows the cut–off frequency f_c, for high optical power levels ($P_i > P_{i0}$), increases with the optical power density P_i, because the potential barrier height Φ_{BL} decreases, leading to a corresponding increase in $\Delta\Phi_{BL}$ and according to eq. (9), to an increase of the cut–off frequency f_c. It must be mentioned that according to eq.(11) P_{i0} depends exponentially on V_R whereas depends linearly on λ. Typical value of P_{i0} for V_R=-6V and for λ in the range from 0.35μm to 0.75μm is about $2.5{\cdot}10^{-4}$ W/cm^2.

For very high incident optical power levels ($P_i >> 10^{-1}$W/cm^2), the cut–off frequency, for all the curves, is possibly saturated. This effect can be attributed to the abrupt saturation of the trapped electron density. More specifically as the electron density n^*_{B0} approaches closely the donor concentration N_B the energy band well becomes very shallow, and losses the ability to accumulate photogenerated electrons. Also, for low optical power levels ($P_i \le P_{i0}$), the cut– off frequency f_c shows to be independent from the optical power density P_i, which is in agreement with eq.(12). This happens because; at very low optical power levels ($P_i \le P_{i0}$) the density of the accumulated electrons in the middle layer is very small compared to the donor

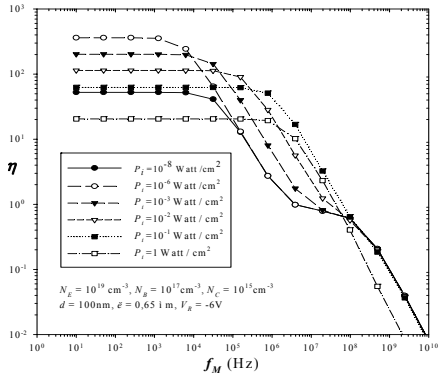

Fig. 3. S-PISCES-LUMINOUS simulation results of the external quantum efficiency, η_{ext}, , as a function of the light modulation frequency, f_M, ,for different values of the optical power density, P_i.

density, N_B, so that the total charge density in the middle layer $Q(x)$, which determines the barrier height, remains unchanged. As P_i increases, the density of the accumulated electrons becomes gradually significant, so that $Q(x)$ begins to decrease. This leads to a decrease in the Φ_{BL} and, consequently, to an increase in the barrier lowering $\Delta\Phi_{BL}$. It is obvious from this figure that the curves are straight lines over a certain range of optical power densities.

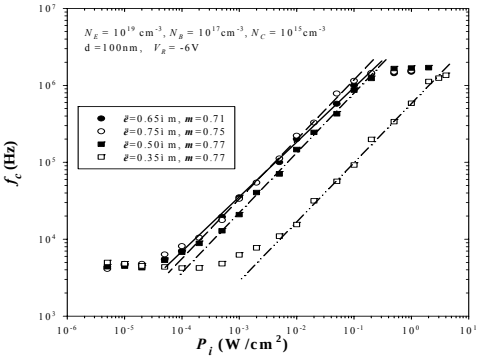

Fig. 4. S- PISCES- LUMINOUS simulatio n results of the cut – off frequency, f_c,, as a function of the incident optical power density, P_i , falling on the BBD.

The linear part, in all curves, indicates that the cut–off frequency increases, in a log–log scale, as the incident optical power density increases with a slope equal to m. The slopes of the linear part of these curves, which are all almost equal to 0.7, are close to the value of the factor m,

as it was found in a previous work [12]. This value of m denotes that it is not clear which is the dominant transport mechanism. Possibly, both of them coexist.

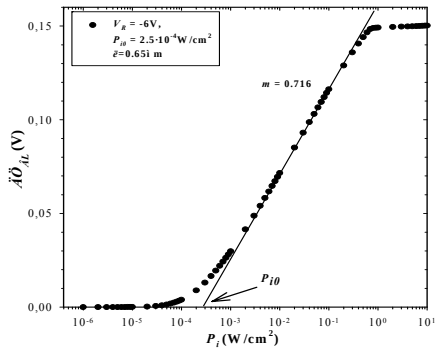

Fig. 5. S-PISCES-LUMINOUS simulation results of the device barrier lowering $\Delta\Phi_{BL}$ as a function of the incident optical power density,P_i falling on the BBD, for a V_R = -6V.

Fig. 5 shows simulation results of the device barrier lowering $\Delta\Phi_{BL}$, obtained from the S-PISCES and LUMINOUS data, as a function of optical power density P_i, for the same BBD structure. The value of factor m as calculated in this figure is $m \approx 0.72$ and is in a good agreement with the slopes calculated in Fig. 4.

The influence of the applied reverse bias voltage V_R, on the cut–off frequency was also investigated. Fig. 6 shows the simulation results of the cut–off frequency f_c, of a BBD, obtained from the S-PISCES and LUMINOUS data, as a function of the applied reverse bias voltage V_R, under pulse illumination for different values of λ. The optical power density was chosen equal to P_i=5·10^{-5} W/cm^2, because this is a convenient value in the linear part of the curves (fig.(3)). It is obvious from this figure that the cut–off frequency *fc*, increases as the reverse bias voltage V_R, increases too. The potential barrier height Φ_{BL} decreases [9] with the

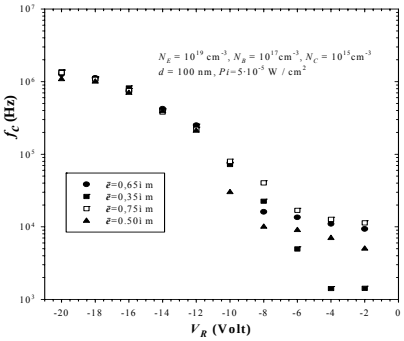

Fig. 6. S- PISCES- LUMINOUS simulation results of the cut – off frequency f_c, of a BBD, as a function the applied reverse bias voltage, V_R, under pulse illumination.

reverse bias voltage, this leads to an increase of J_{diff} and J_{rec} (eq. (7), (8)) and consequently, according to eq.(12), to an increase of f_c. As V_R continues to raise, the cut–off frequency f_c, gradually saturates. This happens because, from the specific value of V_R and beyond, the decrease rate of the barrier height Φ_{BL} also saturates [9].

The simulation results show that high cut–off frequencies can be achieved under specific operational conditions.

4. Conclusions

In this paper we present an extensive study of the transient optical response of silicon Bulk–Barrier Diodes (BBDs). With the device simulation as a basic tool, the influence of significant quantities on the optical response speed of silicon BBDs was investigated. Analytical expressions have been given for the cut–off frequency of silicon BBDs as a function of the applied bias voltage and the light power density. The device simulation played a very important role in a better understanding of the behavior of BBDs, under pulse illumination conditions, because it could easily take into account parameters strongly affecting the behavior of BBD's, e.g. the free carrier presence in the depletion regions. The proposed analytical model described well by the simulation results.

More specifically, the main conclusions of this work can be summarized as follows:

- The incident optical power density strongly affects the cut–off frequency.
- The applied reverse bias influences the cut–off frequency.
- The relatively low cut-off frequencies BBDs obtained from the simulation results are closely associated with the lifetime of accumulated carriers in the middle layer. Consequently, an increase of the optical response speed can be achieved only by trading - off gain.

References

[1] S. M. Sze, High-Speed Semiconductor Devices, Wiley Interscience, 1990.
[2] C. M. Sun et al., Nucl. Instr. And Meth. In Phys. Research A **546**, 437 (2005).
[3] Mader, H., IEEE Trans. On Elect. Dev., **ED-29** (11), 1766 (1982).
[4] N. Georgoulas, IEEE Electron Device Lett., **EDL-3**, 61 (1982).
[5] N. Georgoulas, IEE Proc., **134**, Pt. I, No.5, 153 (1987).
[6] N.Georgoulas, AEU Band 43, Heft 6, 381, (1989).
[7] Q. Zhu, J. Sterzel, B. Schneider, S. Coors, M. Bohm, J. Appl. Phys., **83**(7), 3906 (1998).
[8] H. Son, J. Park, S. Hong, S. J. Jo and J.I. Song, Appl. Phys. Let., **79**(4), 455 (2001).

[9] P. Papadopoulou, N. Georgoulas, L. Georgopoulos, and A. Thanailakis, Electrical Eng. Archiv für Elektrotechnik, **83** (4), 203 (2001).
[10] Van Tuyen, V. Zhirun Hu Rezazadeh, A.A. Yunhong Wu, Electronics Letters, **38**(20), 1228 (2002).
[11] J. Park, S. J. Jo, S. Hong, and J.I. Song, Solid – State Electronics, **46**, 651 (2002).
[12] P. Papadopoulou, N. Georgoulas, and A. Thanailakis, Thin Solid Film, **415**, 276 (2002).
[13] Der-Feng Guo, IEEE Journal Of Quantum Electronics, **40**(4), 413 (2004).
[14] Der-Feng Guo, IEEE Electron Device Letters, **27**(1), 37 (2006).
[15] Der-Feng Guo, et al. Jour. of the Electrochemical Society, **154**(1), H13 (2007).
[16] Abramowitz, M., Stegun, I.A., "Handbook of Mathematical Functions with Formulas, Graphs, and Mathematical Tables", U.S. Department of Commerce, (2002).
[17] R.C. Dorf, "The Electrical Engineering Handbook", C.R.C. Press, p. 113 (2000)

*Corresponding author: ppapado@teikav.edu.gr, lgeorgop@otenet.gr